Journal of Chromatography A, 1200 (2008) 55–61

Contents lists available at ScienceDirect

Journal of Chromatography A

journal homepage: www.elsevier.com/locate/chroma

Monolithic porous polymer stationary phases in polyimide chips for the fast high-performance liquid chromatography separation of proteins and peptides

Pavel A. Levkin[a], Sebastiaan Eeltink[a,1], Thomas R. Stratton[b], Reid Brennen[c], Karla Robotti[c], Hongfeng Yin[c], Kevin Killeen[c], Frantisek Svec[d], Jean M.J. Fréchet[a,d,*]

[a] College of Chemistry, University of California, Berkeley, CA 94720-1460, USA
[b] School of Materials Engineering, Purdue University, 701 W. Stadium Avenue, West Lafayette, IN 47907, USA
[c] Agilent Laboratories, Molecular Technology Laboratory, Santa Clara, CA, USA
[d] The Molecular Foundry, E.O. Lawrence Berkeley National Laboratory, Berkeley, CA 94720, USA

ARTICLE INFO

Article history:
Available online 15 March 2008

Keywords:
Microfluidics
HPLC
Chip
Monoliths
Stationary phase
Protein separation
Peptide separation
Proteomics

ABSTRACT

Poly(lauryl methacrylate-*co*-ethylene dimethacrylate) and poly(styrene-*co*-divinylbenzene) stationary phases in monolithic format have been prepared by thermally initiated free radical polymerization within polyimide chips featuring channels having a cross-section of 200 μm × 200 μm and a length of 6.8 cm. These chips were then used for the separation of a mixture of proteins including ribonuclease A, myoglobin, cytochrome *c*, and ovalbumin, as well as peptides. The separations were monitored by UV adsorption. Both the monolithic phases based on methacrylate and on styrene chemistries enabled the rapid baseline separation of most of the test mixtures. Best performance was achieved with the styrenic monolith leading to fast baseline separation of all four proteins in less than 2.5 min. The *in situ* monolith preparation process affords microfluidic devices exhibiting good batch-to-batch and injection-to-injection repeatability.

1. Introduction

Proteomics is a rapidly emerging field focusing on the nature, function, localization, and posttranslational modifications of all expressed proteins in an organism [1]. Due to the complexity of proteomes and the small quantities of samples typically available, microsystems that afford high sensitivity, rapid throughput, and excellent reproducibility [2–4] must be designed to carry out the proteomic analysis. In this context, microfluidic systems integrating all parts of the separation device into a single chip are particularly attractive.

The first microfluidic device for liquid chromatography (LC) was demonstrated by Ocvirk et al. [5] in the mid 1990s. As might be expected of such an early prototype, the performance of this device featuring a channel packed with C18 particles did not match that of standard high-performance liquid chromatography (HPLC) columns. The use of LC in a micro separation system is attractive as it meets most of the requirements of sensitivity, throughput, and reproducibility while also providing for a wide diversity of separation media to enable separations in a variety of modes. However, the pressurized flow typically used with LC separation systems requires that the chips packed with a classical LC medium consisting of small beads resist the high pressures required during analysis. In general, microfluidic devices can improve separation performance by integrating the injection loop with the separation channel filled with the stationary phase and a MS interface within a single chip thus reducing external contributions to band broadening. Additional benefits of microfluidic technologies, resulting from the small column dimensions, are an increase in sensitivity of detection due to the decrease in sample dilution and a reduction in the generation of waste solvents [6]. For example, an HPLC chip integrating a sample enrichment pre-column, a C18 reversed-phase analytical column, and a nano electrospray tip [4] afforded a significant improvement in performance in the separation of a tryptic digest when compared to a nanoLC/MS/MS system. This microchip also enabled a significant reduction in the sample size and a notable improvement in sensitivity and speed [7].

Chips fabricated from synthetic polymers have recently gained in popularity due to the simplicity of the processes such as injection molding or hot embossing used for their mass-production. They also possess a significant cost advantage when compared to their counterparts made of glass, quarts, or silica [8–13]. In 2005, Agilent Technologies introduced the first polymeric HPLC chip integrating an injection loop, an analytical column, and a nano electrospray

* Corresponding author at: College of Chemistry, University of California, Berkeley, CA 94720-1460, USA. Tel.: +1 510 643 3077; fax: +1 510 643 3079.
E-mail address: frechet@berkeley.edu (J.M.J. Fréchet).
[1] Present address: Dionex, 1046 AA Amsterdam, The Netherlands.

0021-9673/$ – see front matter © 2008 Elsevier B.V. All rights reserved.
doi:10.1016/j.chroma.2008.03.025

interface to a mass spectrometer [12]. This HPLC chip is made by laser ablation of polyimide layers followed by their lamination. There are no fittings, adapters, connectors, or any other dispersive elements, which are prone to leaking and can deteriorate the chromatographic performance of classical capillary nano-LC systems [12,13].

The application and some advantages of the polyimide HPLC chip packed with silica particles over conventional capillary nano-LC systems have been demonstrated for a variety of different analyses [7,13]. Although the HPLC chip is a plastic device it can withstand pressures of up to 20 MPa. Furthermore, excellent peptide recovery was observed due to the inertness of the polyimide material in contrast to fused-silica microparticulate columns [7,13].

The porous polymer monolithic materials that have emerged in the early 1990s [14,15] have become popular as stationary phases for HPLC and capillary electrochromatography (CEC) [16–18]. One of the inherent advantages of monoliths over packed materials, in terms of their chromatographic performance, is the ability to achieve higher porosity of the monolith that enables higher linear flow velocities and hence provides faster separations. In addition, monoliths usually display lower resistance to mass transfer and, as a result, higher efficiencies can be achieved at higher flow rates. This is in sharp contrast to the classical packed materials for which efficiency usually decreases as the flow rate increases [16,18].

Other advantages of the monoliths include the possibility of an *in situ* preparation, which removes the constraints related to size and geometry of the channel to be filled with the porous media. This is especially important for the implementation of the microfluidic approach, where the channel geometry can be fairly complicated in order to accommodate different functional components in a compact chip [19,20].

Different liquid precursors have been used for the preparation of polymer-based monolithic stationary phases [16–18,21–23]. Monomers such as acrylamide [23], styrene, divinylbenzene [24,25], as well as various acrylates [26], methacrylates [27–30], and norbornene [31] have all been used. The morphology of the monolithic polymer is strongly affected by both the composition of the polymerization mixture and the conditions under which the polymerization process is carried out [21,28,29]. The different monoliths have thus been optimized for specific applications by tuning them with a wide range of functionalities [29,32,33], among which hydrophobic [27,28,34] hydrophilic [35], ionizable [28,34], and reactive [36,37] are the most frequently used.

Monoliths are ideally suited for use as components in microfluidic systems [38] as a result of their great flexibility in terms of chemical functionality and of the morphology that can be achieved readily during *in situ* preparation. Numerous functional modules for different applications in microfluidic formats, such as pre-concentration and solid-phase extraction (SPE) [39,40], micro reactors [36,41], mixers [42], stationary phases [29] and valves [43] have already been reported.

The present work targeting the design of a monolithic stationary phase for a novel Agilent polyimide HPLC chip coupled to a UV detector has involved the *in situ* preparation of both methacrylate- and polystyrene-based monoliths and their testing in the separation of protein and peptide mixtures.

2. Experimental

2.1. Chemicals

Lauryl methacrylate (LaMA), ethylene dimethacrylate (EDMA), styrene (ST), divinylbenzene (DVB), 1-decanol, tetrahydrofuran (THF), 2,2′-azobisisobutyronitrile (98%, AIBN), 1,4-butanediol (99%), 1-propanol (99%), methanol (99%), basic alumina, pre-packed column for removing inhibitors, acetonitrile (HPLC grade), methanol (HPLC grade) water (LC–MS grade), formic acid (LC–MS grade), ribonuclease A (85%, from bovine pancrease), myoglobin (≥90%, from horse heart), cytochrome *c* (from bovine heart), ovalbumin (99%, grade VI, from chicken egg), Ala-Ala, Tyr-Gly-Gly, methionine enkephalin, lutenizing hormone releasing hormone (LHRH), alytesin and somatostatin were purchased from Sigma–Aldrich (St. Louis, MO, USA). Tryptic digest of cytochrome *c* was purchased from Michrom Bioresources (Auburn, CA, USA).

EDMA, ST, and DVB were purified by passage through a layer of activated basic alumina followed by distillation under reduced pressure. LaMA was purified by passing it through a commercial pre-packed column for the removal of inhibitors.

2.2. HPLC chip design and instrumentation

A prototype microfluidic HPLC chip, designed to enable UV detection and consisting of several laminated layers of polyimide with laser-ablated channels [13], was fabricated at Agilent Laboratories (Santa Clara, CA, USA). Fig. 1 shows the channel layout that includes a 68 mm long separation channel with a 200 μm × 200 μm square cross-section, an injection loop with a volume of 40 nL, waste channel, and alignment holes. An Agilent 1100 Series nanopump was attached to the chip using a 25 μm i.d. fused silica capillary. The chip was sandwiched between the stator and rotor of a two-position valve [13] and aligned with the 80 nL flow cell of a modified 1100 series Agilent UV detector while monitoring adsorption at 210 nm. During injection, the rotor was positioned to enable syringe loading of the sample into the injection channel. Simultaneously, the stationary phase in the separation channel was conditioned with the mobile phase delivered by the Agilent nanopump. Injection of the sample and subsequent separation were started by switching the rotor to the position connecting the nanopump, injection loop to the separation channel.

Scanning electron micrographs of cross-sections of the channels and monoliths inside were obtained using the Zeiss Gemini Ultra-55 Analytical Scanning Electron Microscope. Optical microscopy images were acquired using the inverted Nikon Eclipse TE200 microscope.

2.3. In situ preparation of monolithic stationary phases

Porous polymer monoliths were prepared by thermally initiated free radical polymerization using AIBN as the initiator. The

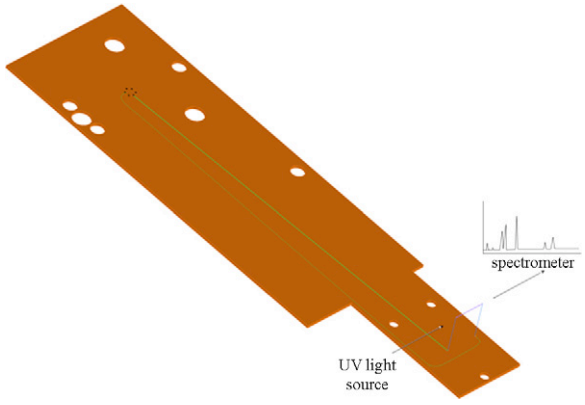

Fig. 1. Schematic layout of microfluidic polyimide chip with integrated LC monolith column and exit ports for UV absorbance detection. The wide line shows the LC separation column. The thin line shows the return channel. These channels are connected through the off-chip UV detection cell (cross-section 120 μm × 120 μm; length 6 mm). The UV cell itself is not shown to simplify the scheme.

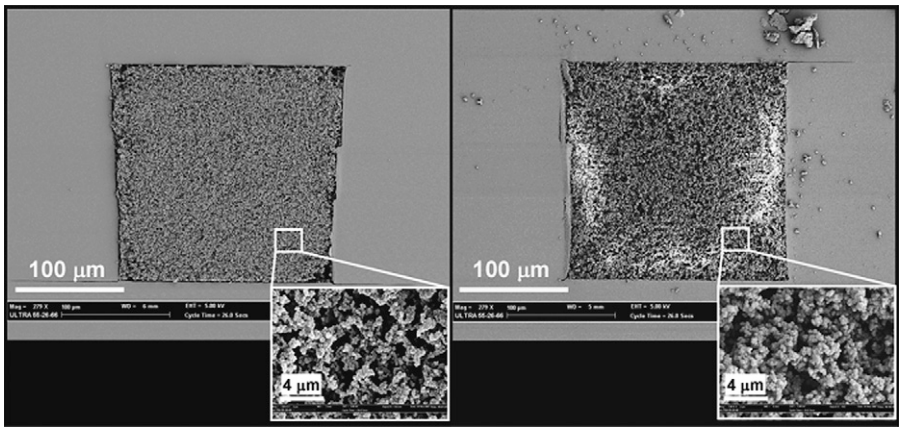

Fig. 2. SEM images of the cross-section of the separation channel in a polyimide HPLC chip filled with poly(lauryl methacrylate-*co*-ethylene dimethacrylate) (left) and poly(styrene-*co*-divinylbenzene) monolith (right).

methacrylate-based monolith was prepared from a mixture of lauryl methacrylate (24.0%, w/w), ethylene dimethacrylate (16.0%, w/w), 1-propanol (45.5%, w/w), 1,4-butanediol (14.5%, w/w) and AIBN (1%, w/w, with respect to monomers) [27]. The styrene-based monolith was prepared using the published procedure [25] from a mixture of styrene (20.3%, w/w), divinylbenzene (20.5%, w/w), 1-decanol (51.2%, w/w), tetrahydrofuran (8.0%, w/w) and AIBN (1%, w/w, with respect to monomers). The polymerization mixtures were de-aerated by purging with a stream of nitrogen for 10 min. The chip was clamped in a home-made device that allowed filling with a syringe. The injection loop and the separation channel can be filled with the polymerization mixture each either separately or simultaneously. The inlets and outlet of the device were then sealed and polymerization was carried out at 70 °C for 24 h in a thermostated bath. Alternatively, the chip containing the polymerization mixture was placed on top of a copper home-made chip-heating device. After completion of the polymerization, the porogens (1,4-butanediol and 1-propanol for methacrylates or 1-decanol and tetrahydrofuran for styrenics) were flushed out with about 100 channel volumes of methanol and the chip was then used directly in the HPLC separations.

2.4. Chromatographic separations

The separations were performed using a gradient of acetonitrile in water (both containing 0.05%, v/v, formic acid) at 30 °C at different flow rates. Sample concentration in water was 0.1–0.2 mg/mL. Data processing was carried out using Agilent 1100 Chemstation software.

3. Results and discussion

3.1. In-chip preparation of monolithic stationary phases

We have previously demonstrated that poly(lauryl methacrylate-*co*-ethylene dimethacrylate) (LaMA–EDMA) monoliths prepared in fused-silica capillaries could be used for the efficient separation of peptides obtained by the tryptic digestion of cytochrome *c* [27]. Poly(styrene-*co*-divinylbenzene) (ST-DVB) monolith represents another stationary phase useful for the separation of peptides and proteins [22–25,44].

Although photoinitiated polymerization is generally preferred for the fabrication of monoliths in chips since it enables photopatterning [32], the technique requires chips fabricated from UV transparent substrates such as cyclic olefin copolymer (COC) [45,46] while the aromatic polyimide chips used in this work absorb strongly in the UV. Therefore, thermally initiated polymerization had to be used for the fabrication of LaMA–EDMA and ST-DVB monoliths in the channels of the polyimide chips. A benefit of thermal polymerization is that it allows the use of UV absorbing, aromatic monomers such as ST and DVB that cannot be used for UV initiated photopolymerization. The SEM micrographs of the cross-section of the separation channels shown in Fig. 2 reveal that the typical interconnected microglobular structure is achieved for both the LaMA–EDMA and the ST-DVB monoliths. The size of the globules formed in the LaMA–EDMA monolith calculated from an average of 50 readings was 125 ± 15 nm. The morphology of the PS-DVB monolith is slightly different with an average microglobule size of 280 ± 30 nm. The SEM micrographs also reveal that both types of

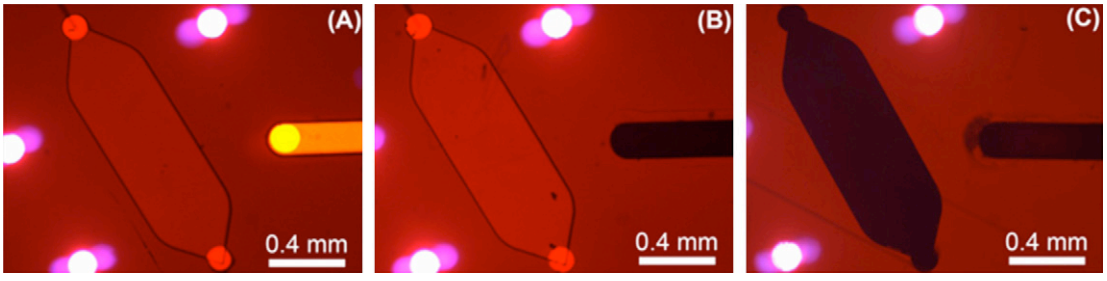

Fig. 3. Optical micrographs of a part of an empty polyimide chip (A), a chip with the injection channel empty and the separation channel filled with the monolith (B), and a chip with both injection and separation channels containing the monolith (C).

monoliths appear to adhere well to the wall surface of the channel. This finding is surprising since the formation of voids is typically observed at the monolith–polymer wall interface unless the surface is functionalized [47].

Both the design of the chip and the device used to fill it facilitate the preparation of monoliths located in either the injection loop or the separation channel as well as simultaneously in both compartments. Fig. 3 shows optical micrographs of an HPLC chip with all channels empty, a chip with a monolith in the separation channel only, and a chip with monolithic structures in both the injection and the separation channels.

3.2. Separation of proteins

3.2.1. Effect of flow rate

The chips containing monolith can be easily attached to the chromatographic system consisting of a pump and UV detector, and used for the reversed phase separation of a mixture of four standard proteins comprising ribonuclease A, myoglobin, cytochrome *c*, and ovalbumin. A key feature of monolithic stationary phases is the presence of large through-pores, which enable convective mass transport that is much faster than diffusion in pores of traditional particulate packings. This accelerated mass transport is particularly valuable in the separation of large molecules for which diffusion is slow. Therefore, the monolithic stationary phases enable high flow velocities without a notable decrease in efficiency of separation. Fig. 4 shows the separations of the test mixture containing four proteins at different flow rates using both LaMA–EDMA and ST-DVB monolithic stationary phases. Clearly, the higher the flow rate, the better the separation with best performance achieved at a flow rate of 4 μL/min, the highest flow-rate achievable with the Agilent nanopump. A comparison of the separations with the two monolithic stationary phases indicates that better separations with narrower peaks are achieved using the chip containing the ST-DVB monolith. The higher efficiency of the ST-DVB monolith can be attributed to an optimal combination of surface chemistry and porosity. The presence of voids in the structure at the monolith–wall interface may be another reason for the lesser performance of the LaMA–EDMA monolith though it must be emphasized that no such voids were detected in the SEM micrographs.

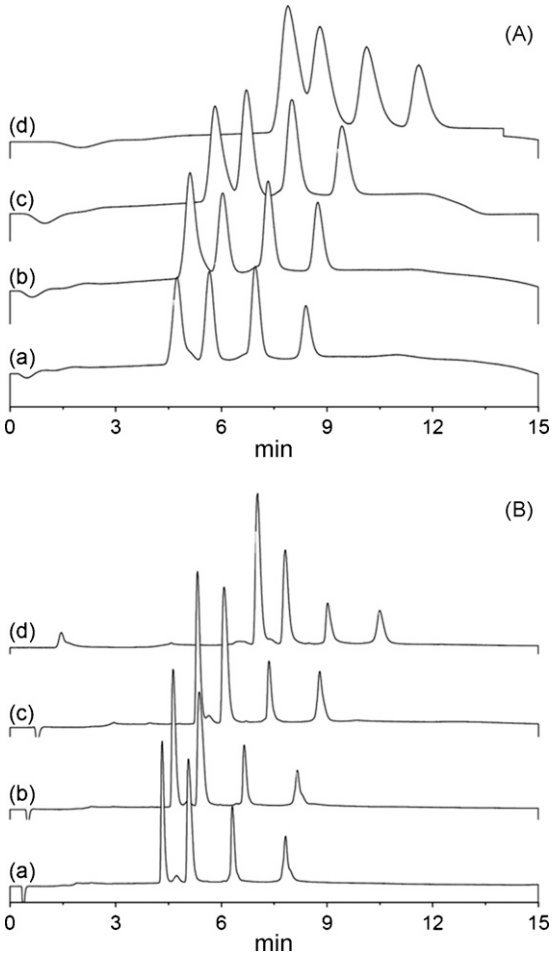

Fig. 4. On-chip separations of ribonuclease A, cytochrome *c*, myoglobin, ovalbumin (order of elution) using the monolithic poly(lauryl methacrylate-*co*-ethylene dimethacrylate) (A) and poly(styrene-*co*-divinylbenzene) (B) stationary phases at different flow rates: (a) 4, (b) 3, (c) 2, and (d) 1 μL/min. Gradient: 0–60% of acetonitrile in water (0.05%, v/v, of formic acid) in 10 min. Concentration of proteins in sample solution: 0.2 and 0.1 mg/mL for poly(lauryl methacrylate-*co*-ethylene dimethacrylate) and poly(styrene-*co*-divinylbenzene) monoliths, respectively. Injection volume 40 nL. Detection: UV at 210 nm.

3.2.2. Effect of gradient steepness

Initially, the separations were carried out using a shallow gradient and the flow rate of 4 μL/min that had previously been found to afford best separations. Although both types of monolithic stationary phases could achieve baseline separation as shown in Fig. 5, the run times were too lengthy to make these separations practical. Therefore the separation process was accelerated by decreasing the gradient time, thus increasing the gradient steepness. As seen in Fig. 5, this approach leads to a significant decrease in run times.

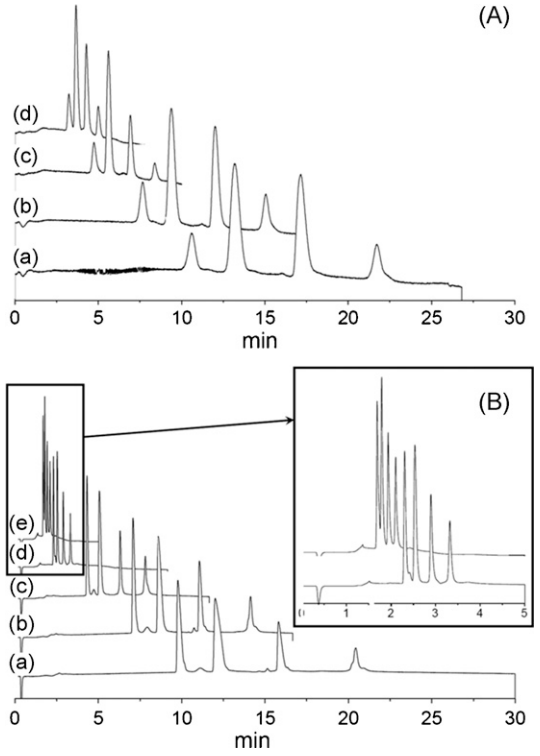

Fig. 5. On-chip separations of ribonuclease A, cytochrome *c*, myoglobin, ovalbumin (order of elution) using the monolithic (A) poly(lauryl methacrylate-*co*-ethylene dimethacrylate) and (B) poly(styrene-*co*-divinylbenzene) stationary phases. Gradient of the mobile phase: 0–60% of acetonitrile in water (0.05%, v/v, of formic acid) in (a) 30, (b) 20, (c) 10, and (d) 5 min, and 0–100% of acetonitrile in water (0.05%, v/v, of formic acid) in (e) 2 min. Concentration of proteins in sample solution: 0.1 mg/mL. Injection volume 40 nL. Flow rate: 4 μL/min. Detection: UV at 210 nm.

For example, a 5 min gradient of 0–60% acetonitrile in aqueous formic acid affords a baseline separation of the proteins in less than 5 min using the chip containing the LaMA–EDMA monolith. Similarly, the chip with ST-DVB monolith separates all four proteins in about 2.5 min using a 2 min gradient of 0–100% acetonitrile in aqueous formic acid. Overall, an increase in the mobile phase gradient steepness significantly decreases the run time while preserving the baseline separation profile. Once again, the ST-DVB monolith performed better and excellent separations were achieved even with the very steep gradients.

3.3. Separation of peptides

Separation and characterization of peptides, typically obtained by digestion of proteins, is a requirement for most proteomic protocols. Therefore, peptides were also used to evaluate the performance of the chips containing the poly(styrene-*co*-divinylbenzene) monolithic stationary phase. Fig. 6A shows the baseline separation of a mixture containing five peptides: Tyr-Gly-Gly, [Ala^2]-methionine-enkephalin, LHRH, alytesin, and somatostatin, with molecular masses ranging from 300 to 3000 in less than 4 min. Fig. 6B then presents the separation of a tryptic digest of cytochrome *c*. Although the complex mixture of the peptides appears to be separated according to the UV trace, an exact assignment of the peptides could not be achieved since a mass spectrometric detector was not available with this instrumental set-up.

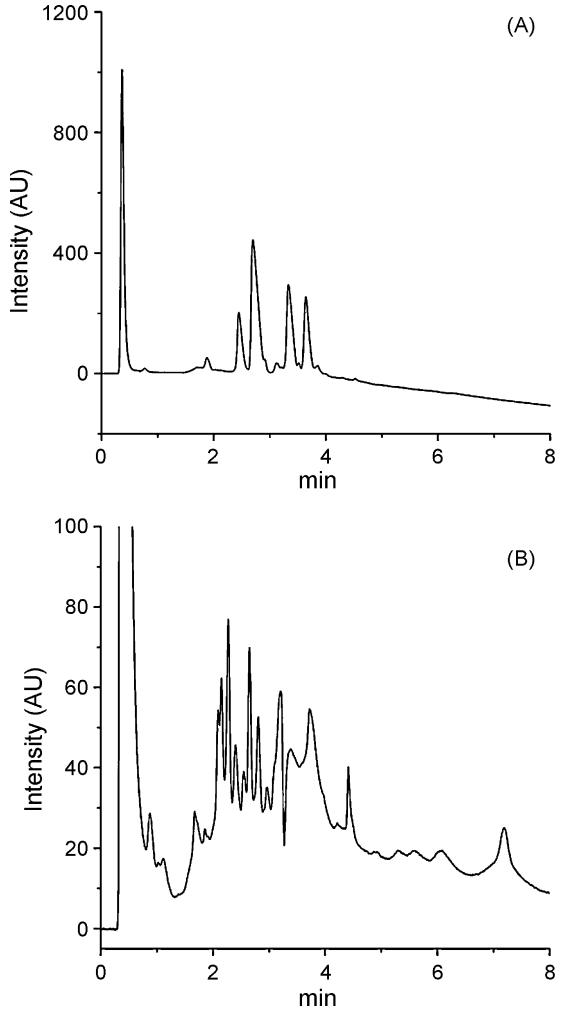

Fig. 6. On-chip separation of a mixture of peptides Tyr-Gly-Gly, [Ala^2]-methionine-enkephalin, LHRH, alytesin, and somatostatin (elution order) (A) and of a tryptic digest of cytochrome *c* (B) using the monolithic poly(styrene-*co*-divinylbenzene) stationary phase. Gradient: 0–60% of acetonitrile in water (0.05%, v/v, of formic acid) in 7 min (A) and 10 min (B). Concentration of peptides in sample solution: 0.1 mg/mL. Injection volume 40 nL. Flow rate: 4 μL/min. Detection: UV at 210 nm.

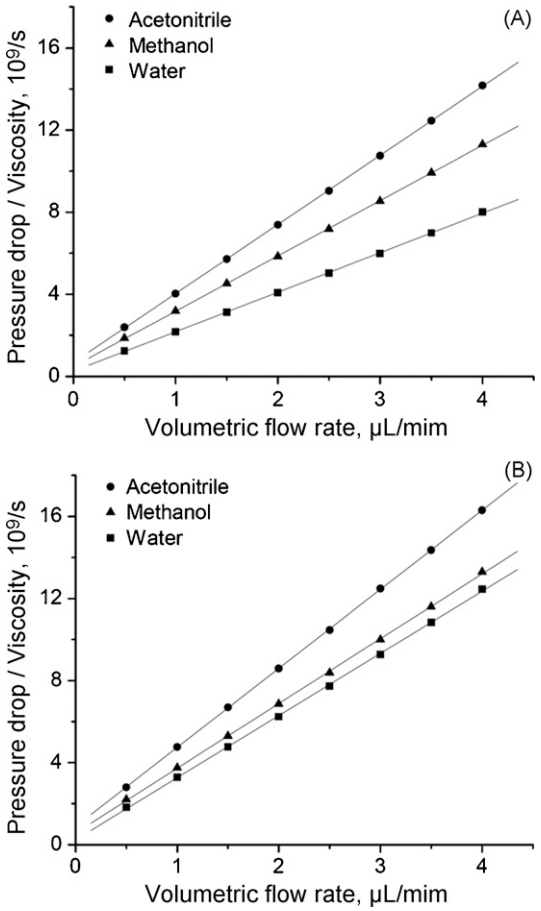

Fig. 7. Pressure drop in the polyimide chip normalized by viscosity of the solvent as a function of flow rate of acetonitrile, methanol, and water through channel containing poly(lauryl methacrylate-*co*-ethylene dimethacrylate) (A) and poly(styrene-*co*-divinylbenzene) monolith (B).

3.4. Permeability, stability, and repeatability

The permeability calculated using superficial velocity-based, $k_{p.F.}$, [16] was found to be 1.4×10^{-10} and 6.3×10^{-11} cm^2 for the LaMA–EDMA and ST-DVB monoliths, respectively. Based on these values, the permeability of the LaMA–EDMA monolith appears to be similar to that of columns packed with ca. 4 μm silica particles, while the permeability of the ST-DVB monolith resembles that of columns containing 2–3 μm particles. Fig. 7 shows the pressure drop normalized for differences in solvent viscosity at 25 °C as a function of flow rate. Water, methanol, and acetonitrile are the typical components of mobile phases in reversed phase separations. The linearity of the pressure drop vs. the flow rate plot confirms both the good mechanical strength of the monoliths and the absence of any compression even at the flow rate of 4 μL/min. The highest pressure drop for both monoliths was observed with acetonitrile. This is indicative of a reduction in pore size possibly due to swelling of the microglobules due to interactions of the monolith with acetonitrile.

Table 1
Repeatability of protein separations using poly(lauryl methacrylate-*co*-ethylene dimethacrylate) and poly(styrene-*co*-divinylbenzene) monoliths in microfluidic chip

	Ribonuclease A		Ovalbumin	
	t_R[a]	w_h[b]	t_R	w_h
Poly(lauryl methacrylate-co-ethylene dimethacrylate) monolith				
Mean, $n = 10$ (s)	193.8	13.0	298.7	11.8
RSD (%)	0.5	4.0	0.1	4.6
Confidence interval, 95% (s)	193.78–193.82	12.99–13.01	298.69–298.71	11.79–11.81
Poly(styrene-co-1,4-divinylbenzene) monolith				
Mean, $n = 10$ (s)	173.8	3.3	275.8	4.9
RSD (%)	0.3	4.6	0.3	1.9
Confidence interval, 95% (s)	173.79–173.81	3.297–3.303	275.78–275.82	4.898–4.902

Conditions: Mobile phase gradient: 0–60% acetonitrile in water (0.05%, v/v, of formic acid) in 10 min. Flow rate: 4 μL/min. UV detection at 210 nm. Concentration of proteins in sample 0.2 mg/mL and 0.1 mg/mL for poly(lauryl methacrylate-*co*-ethylene dimethacrylate) and poly(styrene-*co*-divinylbenzene), respectively.
[a] Retention time, s.
[b] Peak width at half height, s.

Fig. 8 shows 10 overlaid chromatograms obtained by successive gradient separations of four proteins on both the LaMA–EDMA and the ST-DVB monolithic stationary phases. The match of both retention times and peak widths demonstrates an excellent run-to-run repeatability. Table 1 presents the average retention times, relative standard deviations, and confidence interval for ribonuclease A, eluting first, and ovalbumin, eluting as the last peak, on both monolithic stationary phases. The deviations are very small as characterized by relative standard deviations in the range of 0.1–0.5%.

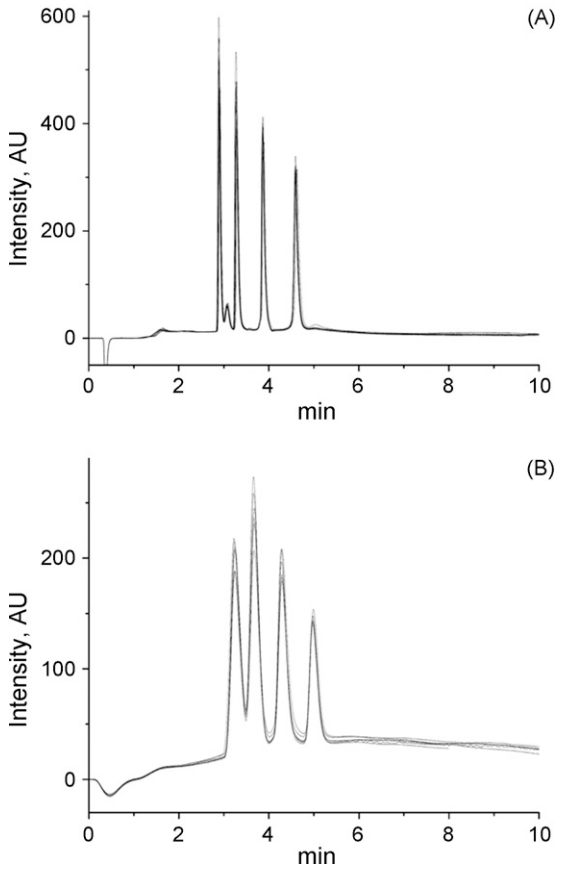

Fig. 8. Overlaid chromatograms obtained by 10 successive gradient separations of ribonuclease A, cytochrome *c*, myoglobin, ovalbumin (order of elution) using chips containing both monolithic poly(styrene-*co*-divinylbenzene) (A) and poly(lauryl methacrylate-*co*-ethylene dimethacrylate) (B) stationary phases. Gradient: 0–60% of acetonitrile in water (0.05%, v/v, of formic acid) for 10 min. Concentration of proteins in sample solution: 0.2 and 0.1 mg/mL for poly(lauryl methacrylate-*co*-ethylene dimethacrylate) and poly(styrene-*co*-divinylbenzene) monoliths, respectively. Injection volume 40 nL. Flow rate: 4 μL/min. Detection: UV at 210 nm.

4. Conclusions

This preliminary study demonstrates that both methacrylate-based and styrene-based monolithic stationary phases can be prepared in the polyimide HPLC chip using thermally initiated free radical polymerization. This polymerization enables the preparation of monoliths with a wide variety of chemistries since the UV transparency requirement operative for photoinitiated polymerization is not an issue. Both types of the monoliths afford efficient separation of proteins within a short period of time using a steep gradient of the mobile phase.

Our approach will also allow the preparation of monolith with different chemistries in different compartments of the chip that can be independently filled with polymerization mixtures differing in composition. This may then enable the design and fabrication of microfluidic devices that will combine functions such as preconcentration or digestion and separation in the same chip without being affected by the shape and length of the separation channel, and, given the flexibility of the polyimide chip preparation technique, it is possible to envision the implementation of several different functional blocks in a single chip.

To achieve the same the quality of separation in a shorter period of time via increasing the gradient steepness, the gradient volume defined as the product of gradient time by flow rate should be kept constant. This means that a decrease in gradient time has to be compensated by an increase in flow rate. While it is likely that higher flow rates can further improve the quality of the separations, our current setup did not allow us to test the use of higher flow velocities to demonstrate even faster separation and the only variable we could change was the gradient steepness. Another option to further increase the speed and efficiency of the HPLC analyses in the chip would be to decrease the channel cross-section leading to an increase in flow velocity at a specific flow rate. However, this approach necessitates a reduction in the volume of the UV detector cell from the current 80 nL of the commercially available Agilent cell used in these experiments to a much smaller size to minimize significant detection related dispersion.

Acknowledgements

Support of this research by a grant of the National Institute of Biomedical Imaging and Bioengineering, National Institutes of Health (EB-006133) is gratefully acknowledged. Measurement work at the Molecular Foundry was supported by the Director,

Office of Science, Office of Basic Energy Sciences, Division of Materials Sciences and Engineering, of the US Department of Energy under Contract No. DE-AC02-05CH11231. T.S. is grateful to the US Department of Homeland Security for a scholarship. Agilent Technologies, Inc. is acknowledged for kindly supplying chip-related instrumentation and Debbie Ritchey at Agilent Laboratories is thanked for fabricating the prototype chips we used.

References

[1] M. Hamdan, P.G. Righetti, Proteomics Today, Wiley, Hoboken, NJ, 2005.
[2] J.W. Cooper, Y. Wang, C.S. Lee, Electrophoresis 25 (2004) 3913.
[3] N. Lion, T.C. Rohner, L. Dayon, I.L. Arnaud, E. Damoc, N. Youhnovski, Z. Wu, C. Roussel, J. Josserand, H. Jensen, J.S. Rossier, M. Przybylski, H.H. Girault, Electrophoresis 24 (2003) 3533.
[4] J. Hardouin, M. Duchateau, R. Joubert-Caron, M. Caron, Rapid Commun. Mass Spectrom. 20 (2006) 3236.
[5] G. Ocvirk, E. Verpoorte, A. Manz, M. Grasserbauer, H.M. Widmer, Anal. Methods Instrum. 2 (1995) 74.
[6] P. Sajonz, X. Gong, W.R. Leonard, M. Biba, C.J. Welch, Chirality 18 (2006) 803.
[7] M. Ghitun, E. Bonneil, M.H. Fortier, H. Yin, K. Killeen, P. Thibault, J. Sep. Sci. 29 (2006) 1539.
[8] J.C. McDonald, G.M. Whitesides, Acc. Chem. Res. 35 (2002) 491.
[9] J. Wang, M. Pumera, M.P. Chatrathi, A. Escarpa, R. Konrad, A. Griebel, W. Doerner, H. Loewe, Electrophoresis 23 (2002) 596.
[10] S.K. Sia, G.M. Whitesides, Electrophoresis 24 (2003) 3563.
[11] T.B. Stachowiak, F. Svec, J.M.J. Fréchet, J. Chromatogr. A 1044 (2004) 97.
[12] H. Yin, K. Killeen, R. Brennen, D. Sobek, M. Werlich, T. Van de Goor, Anal. Chem. 77 (2005) 527.
[13] H. Yin, K. Killeen, J. Sep. Sci. 30 (2007) 1427.
[14] F. Svec, J.M.J. Fréchet, Anal. Chem. 64 (1992) 820.
[15] F. Svec, J.M.J. Fréchet, Science 273 (1996) 205.
[16] G. Guiochon, J. Chromatogr. A 1168 (2007) 101.
[17] F. Svec, J. Sep. Sci. 28 (2005) 729.
[18] F. Svec, C.G. Huber, Anal. Chem. 78 (2006) 2100.
[19] H. Audrain, Angew. Chem., Int. Ed. 46 (2007) 1772.
[20] G.M. Whitesides, Nature 442 (2006) 368.
[21] F. Svec, T.B. Tennikova, Z. Deyl (eds.), Monolithic Materials —Preparation, Properties and Applications (Journal of Chromatography Library, vol. 67), Elsevier, Amsterdam, 2003.
[22] C. Viklund, F. Svec, J.M.J. Fréchet, K. Irgum, Chem. Mater. 8 (1996) 744.
[23] S. Hjertén, J.L. Liao, R. Zhang, J. Chromatogr. 473 (1989) 273.
[24] I. Gusev, X. Huang, C. Horváth, J. Chromatogr. A 855 (1999) 273.
[25] A. Premstaller, H. Oberacher, C.G. Huber, Anal. Chem. 72 (2000) 4386.
[26] T. Tegeler, Y. Mechref, K. Boraas, J.P. Reilly, M.V. Novotny, Anal. Chem. 76 (2004) 6698.
[27] S. Eeltink, L. Geiser, F. Svec, J.M.J. Fréchet, J. Sep. Sci. 30 (2007) 2814.
[28] S. Eeltink, E.F. Hilder, L. Geiser, F. Svec, J.M.J. Fréchet, G.P. Rozing, P.J. Schoenmakers, W.T. Kok, J. Sep. Sci. 30 (2007) 407.
[29] S. Eeltink, F. Svec, Electrophoresis 28 (2007) 137.
[30] L. Geiser, S. Eeltink, F. Svec, J.M.J. Fréchet, J. Chromatogr. A 1140 (2007) 140.
[31] B. Mayr, G. Hoelzl, K. Eder, M.R. Buchmeiser, C.G. Huber, Anal. Chem. 74 (2002) 6080.
[32] T. Rohr, E.F. Hilder, J.J. Donovan, F. Svec, J.M.J. Fréchet, Macromolecules 36 (2003) 1677.
[33] T.B. Stachowiak, F. Svec, J.M.J. Fréchet, Chem. Mater. 18 (2006) 5950.
[34] E.F. Hilder, F. Svec, J.M.J. Fréchet, Anal. Chem. 76 (2004) 3887.
[35] T.B. Stachowiak, D.A. Mair, T.G. Holden, L.J. Lee, F. Svec, J.M.J. Fréchet, J. Sep. Sci. 30 (2007) 1088.
[36] D.S. Peterson, T. Rohr, F. Svec, J.M.J. Fréchet, Anal. Chem. 75 (2003) 5328.
[37] X. Dong, J. Dong, J. Ou, Y. Zhu, H. Zou, Electrophoresis 27 (2006) 2518.
[38] D.S. Peterson, Lab Chip 5 (2005) 132.
[39] F. Svec, J. Chromatogr. B 841 (2006) 52.
[40] C. Yu, M.H. Davey, F. Svec, J.M.J. Fréchet, Anal. Chem. 73 (2001) 5088.
[41] T.C. Logan, D.S. Clark, T.B. Stachowiak, F. Svec, J.M.J. Fréchet, Anal. Chem. 79 (2007) 6592.
[42] T. Rohr, C. Yu, M.H. Davey, F. Svec, J.M.J. Fréchet, Electrophoresis 22 (2001) 3959.
[43] Q. Luo, S. Mutlu, Y.B. Gianchandani, F. Svec, J.M.J. Fréchet, Electrophoresis 24 (2003) 3694.
[44] Q. Wang, F. Svec, J.M.J. Fréchet, Anal. Chem. 65 (1993) 2243.
[45] G. Khanarian, Opt. Eng. 40 (2001) 1024.
[46] R.R. Lamonte, D. McNally, Plast. Eng. 56 (2000) 51.
[47] T.B. Stachowiak, T. Rohr, E.F. Hilder, D.S. Peterson, M. Yi, F. Svec, J.M.J. Fréchet, Electrophoresis 24 (2003) 3689.